

1 *Communication*

2 **Catalytic hot gas filtration for tailoring vapor-phase** 3 **chemistry of fast pyrolysis bio-oils**

4 **Mi Lu** ^{1,+}, **Andrew Lepore** ^{2,+}, **Jae-Soon Choi** ¹, **Zhenglong Li** ¹,
5 **Felipe Polo Garzon**², and **Michael Z. Hu** ^{1,*}

6 ¹ Energy and Transportation Sciences Division of Oak Ridge National Laboratory (ORNL);

7 ² Chemical Science Division of Oak Ridge National Laboratory (ORNL)

8

9 + These authors contributed equally to this work.

10 * Correspondence: hum1@ornl.gov; Tel.: 865-574-8782

11

12 **Abstract:** Carboxylic acids such as acetic acid and propionic acid have been investigated as
13 representative components for fast pyrolysis (FP) bio-oil upgrading. Selective catalytic conversion
14 of carboxylic acids can enhance bio-refinery processing economics through catalyst preservation
15 and process intensification. Various metal-doped molybdenum carbide bead catalysts have been
16 synthesized and developed in this work. Our aim is to enable selective conversion of carboxylic
17 acids. In the case of acetic acid conversion, calcium doped Mo₂C beads offer the highest yield of
18 acetone ~96% at 450 °C among undoped and Ca or Ni doped catalysts. By comparing hot gas filter
19 with and without Ca-Mo₂C catalyst tested with real FP vapors, the former showed a 36.7% reduction
20 of acetic acid, a 37.5% reduction of small ketones in aqueous phase, and a ~50% reduction of
21 methoxies (methoxy phenols and methoxy aromatics) in organic phase. The conversion resulted in
22 the formation of more long chain chemicals in the organic phase, which are more amendable for
23 downstream upgrading.

24 **Keywords:** bio-oil; biomass conversion; carbide catalyst; ketonization; doped carbides.

25

26 **1. Introduction**

27 Hot Gas Filtration (HGF) can reduce alkali and alkaline earth metals and solid content from bio-
28 oil, in order to improve vapor composition and protect downstream upgrading and hydrotreatment
29 catalysts from fouling[1]. Packing the catalyst beads to the filter, which becomes Catalytic Hot Gas
30 Filtration (CHGF), can further upgrade bio-oil vapor and provide chemical tailoring of the feed
31 vapors before they enter the downstream upgrading. Among various bio-oil components, carboxylic
32 acids, such as acetic acid and propionic acid, are commonly found in large amounts in bio-oils and
33 contribute to the acidic and corrosive nature of bio-oil[2]. Furthermore, these acids are of low value
34 and present challenges in downstream bio-oil upgrading processes. Small organic acids in liquid bio-
35 oil can catalyze polymerization of reactive species such as sugars and aldehydes during
36 hydroprocessing, cause catalyst fouling, and consume an excessive amount of H₂ producing low-
37 value alkane hydrocarbon gases[3]. This study applied CHGF to address the issues related to
38 carboxylic acids and small carbonyl compounds. The design of CHGF is shown in Figure 1.

39 Various reactions for carboxylic acids on metal or oxide catalysts have been well studied. For
40 instance, hydrodeoxygenation (HDO) of acetic acid produces ethanol[4], decarboxylation (DCO)
41 produces CO₂[5], dehydration yields ethenone[5], reduction produces acetaldehyde[6], and
42 ketonization leads to the production of acetone[7]. The selectivities for these reactions depend
43 strongly on the nature of the catalyst surface. In general, HDO is an attractive route to upgrade bio-
44 oil considering that this process is well established in the petroleum industry; however, HDO of bio-
45 oil usually requires precious metals, high temperatures, and high hydrogen pressures[8]. For
46 example, Huber *et al.* used Ru/C and Pt/C catalysts to produce bi- and tri-cyclic products from phenol

47 with 85% selectivity at 160 °C and 5 MPa hydrogen pressure. The amount of precious metals needed
48 for the degradation of cellulose was relatively high, 4– 10 mg per gram of cellulose [10]. Also, precious
49 metals have a greater tendency towards DCO over HDO, and tend to fully saturate double bonds via
50 hydrogenation. Therefore, it is desirable to develop inexpensive catalysts that can perform carboxylic
51 acid conversion under mild conditions. Interstitial carbides are robust materials which have catalytic
52 properties similar to those of precious metals due to their electronic structure.[10] On the other hand,
53 carbides, such as Mo_2C , have been shown to be more selective towards HDO than DCO as well as
54 have superior stability under upgrading conditions[11–13]. By being less active towards C-C bond
55 scission the hydrocarbons produced typically have greater molecular weight and value[11].

56 Most of the studies on Mo_2C focus on its direct hydrodeoxygenation properties. In this study,
57 we explored the ketonization activity for acetic and propionic acid conversion by modifying Mo_2C
58 with Ca and Ni in catalyst beads form. We found that we could tune the selectivity toward ketone
59 production by doping Mo_2C with Ca. In-situ chemistry tailoring of hot pyrolysis vapors by CHGF
60 platform serves as an alternative processing method to process vapors before they are condensed into
61 bio-oil liquid for more facile subsequent upgrading to hydrocarbon fuels and chemicals. Besides the
62 filtration removal of inorganic mineral (alkali/alkaline metals), catalyst beads-loaded hot gas filters
63 are being developed to enable selective target conversions (such as conversion of carboxylic acids
64 and small carbonyls). Therefore, transforming these carboxylic acids/carbonyls into larger more
65 upgraded molecules before condensation would be beneficial with respect to H and C economy and
66 hydroprocessing catalyst lifetime.



74 **Figure 1.** Schematic pictures of CHGF: Hot gas filtration holder and the filter (left); Packed bed of
75 catalyst beads/pellets inside ceramic filter tube (right).

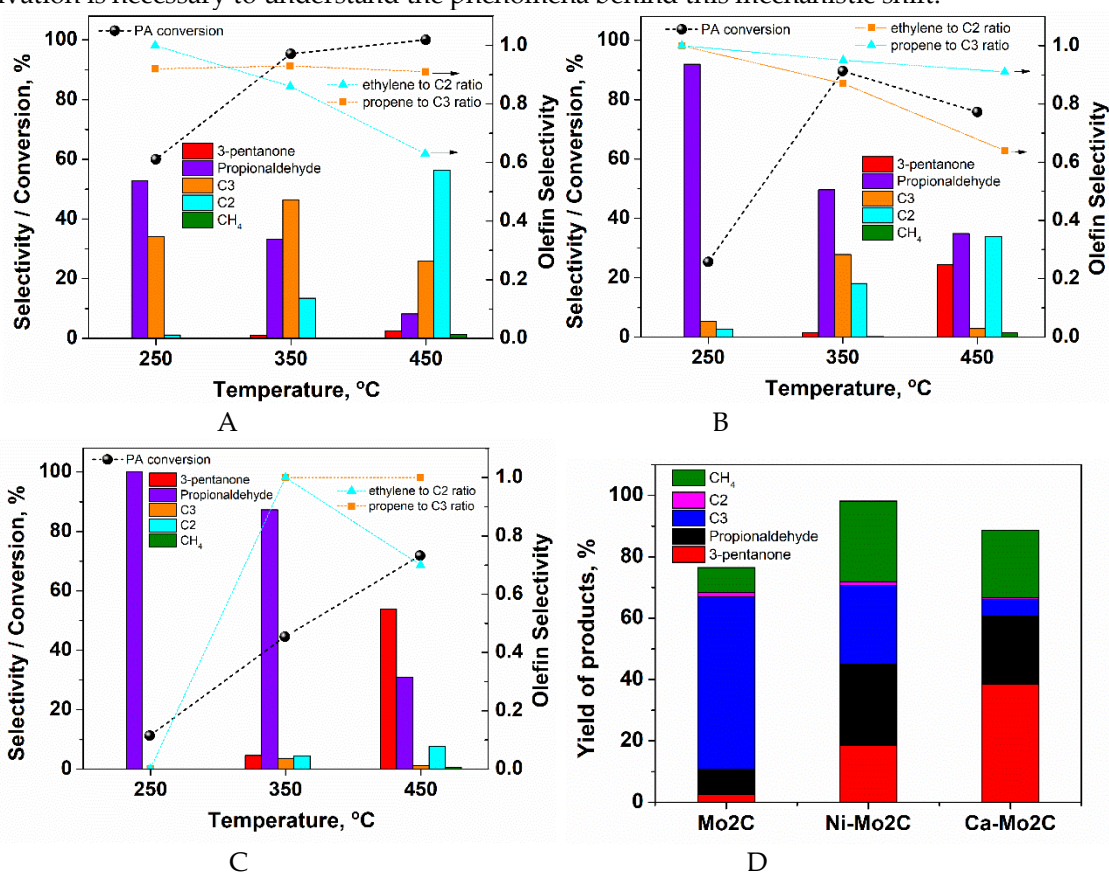
76 2. Results and Discussion

77 Propionic acid conversion and product selectivity was dependent upon reaction temperature for
78 all three Mo_2C catalysts [Figures 2 (A, B and C)]. Un-doped Mo_2C [Figure 2 (A)] had three main
79 products, C3 hydrocarbons (propane and propene), C2 hydrocarbons (ethane and ethylene), and
80 propionaldehyde. At 250 °C, propionaldehyde was the major product (55% selectivity) indicating
81 that hydrogenation was the dominant reaction pathway. The presence of C3 species were also
82 significant at 35% selectivity. The propene could have come from dehydration of 1-propanol
83 produced by propionaldehyde hydrogenation. It is known that Mo_2C surface can possess acidic sites
84 due to the presence of surface oxygen[14]. 1-Propanol, however, was not detected throughout the
85 experiment. This suggests that either 1-propanol dehydration was very fast (i.e., consumed as soon
86 as it formed) or propene was produced by direct hydrogenolysis of the aldehyde carbonyl group[11].
87 C2 products, on the other hand, were negligible. This suggests that cracking or hydrogenolysis
88 reactions were not predominant under these conditions. As the reaction temperature increased from
89 250 to 350 °C, the selectivity shifted away from propionaldehyde to C3 species. The olefin selectivity
90 is the alkene selectivity over the sum of the alkane and alkene species. Propene was ~ 80% of the C3

91 products, indicating that the catalyst had moderate activity toward double bond hydrogenation
 92 under these conditions. A similar trend was observed with C2 species. Increasing the reaction
 93 temperature further to 450 °C drove the selectivity towards C2 species with ethylene being the major
 94 fraction. One possible explanation for this transition is that C-C bond cleavage of propene molecules
 95 became a dominant reaction pathway at high temperatures. However, considering the limited CH₄
 96 formation, its reactivity towards C-C bond cleavage was still relatively modest compared to precious
 97 metal catalysts which would have produced predominantly CH₄ gas at this temperature. Reducing
 98 the temperature back down to 250 °C revealed that the catalyst's activity had significantly decreased
 99 over the experiment, evidenced by the low propionic acid conversion (~5%).

100 Nickel-doped Mo₂C [Figure 2 (B)] was subjected to a slightly different reaction temperature
 101 scheme which was as follows: 250 → 350 → 450 °C. As in the case of Un-doped Mo₂C,
 102 propionaldehyde was the major product. However, selectivity patterns as a function of temperature
 103 presented some substantial differences. This catalyst exhibited a dramatic increase in 3-pentanone at
 104 450 °C as compared with the un-doped catalysts (25 vs. 2.5% selectivity). Interestingly, the 3-
 105 pentanone selectivity was much higher at 350 °C at the end of the experiment than it was in the
 106 beginning (15 vs. 1.5%). On the other hand, the C3 selectivity decreased from 30 to 3% over the course
 107 of the experiment. The olefin selectivity appeared unchanged. This suggests that as the catalyst
 108 became less active towards propionic acid hydrogenation and dehydration (and/or deoxygenation),
 109 the ketonization activity improved. Further investigation into the catalyst acidity and the mode of
 110 deactivation is necessary to understand the phenomena behind this mechanistic shift.

111
 112



113
 114

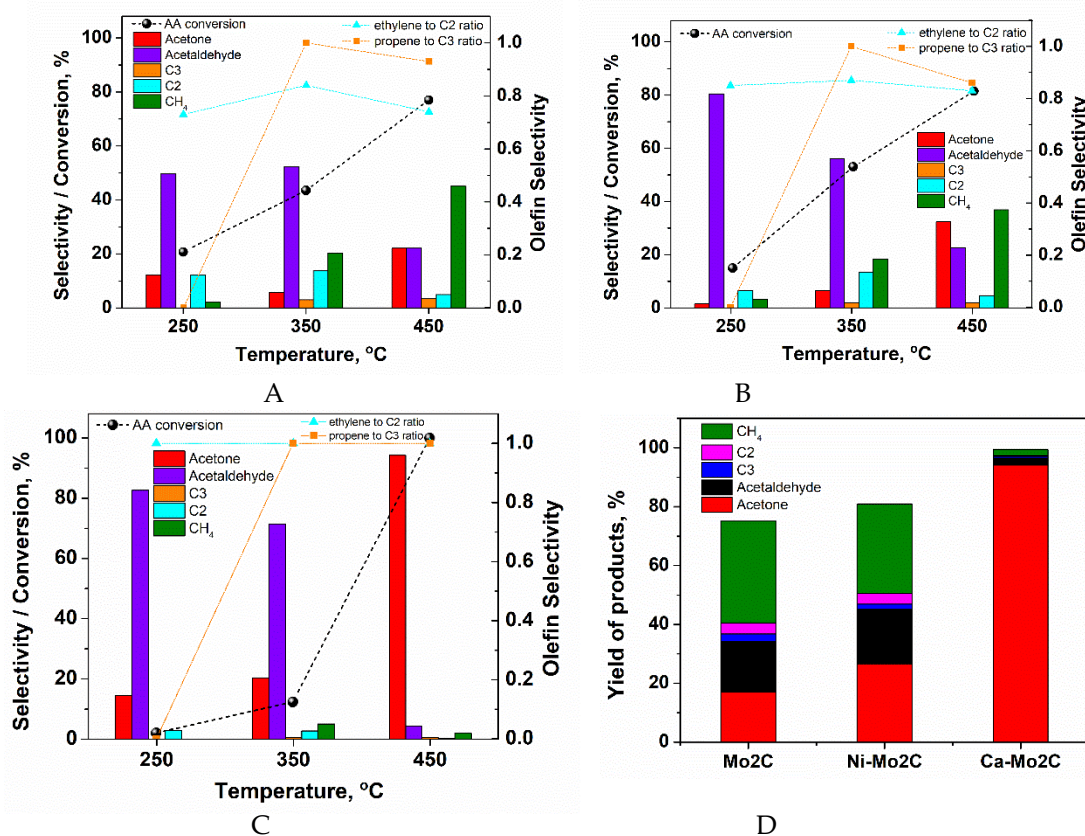
115 **Figure 2.** Product selectivity and of propionic acid conversion over three types of carbide pellet
 116 catalysts after pretreatment with 10% H₂ at 500 °C for 2 h: (A) Mo₂C, 4 h Time On Stream (TOS); (B)
 117 Ni-Mo₂C, 4 h TOS; (C) Ca-Mo₂C, 4 h TOS but *The final injection was taken after running the reaction
 118 for 12 h; (D) Yield of products at 450 °C over three types of carbide catalysts.

119

120 The Ca-doped Mo₂C was subjected to a temperature scheme: 250 → 350 → 450 °C [Figure 3 (C)].
 121 The behavior of the calcium doped Mo₂C was remarkably different from the un-doped and the nickel
 122 doped catalysts. At 250 °C, the catalyst was less active (acid conversion ~ 10%). However, increasing

123 the reaction temperature improved acid conversion monotonously. At low temperatures,
 124 propionaldehyde was again highly favored but at elevated temperatures 3-pentanone was dominant.
 125 The C3 and C2 hydrocarbons remain minor byproducts over the entire temperature range. At 500 °C,
 126 3-pentanone selectivity was 62% and propionic acid conversion was 96%. The reaction was continued
 127 at this temperature for 12 h at which point the 3-pentanone selectivity increased to 83% but the acid
 128 conversion had dropped to 45%. Therefore, the deactivation of Ca-Mo₂C was mainly accompanied
 129 by loss in its hydrogenation function while maintaining its ketonization selectivity.

130 In view of our results of propionic acid hydrodeoxygenation over metal carbides, we reasoned
 131 that acetic acid could go through ketonization to form acetone over metal carbides as well.
 132 Hydrogenation of acetone can lead to 2-propanol which can subsequently be dehydrated to propene.
 133 Hydrodeoxygenation of acetic acid was carried out over un-doped, Ni-, and Ca-Mo₂C. Product
 134 selectivity and acid conversion as a function of reaction temperature are summarized in Figures 3 (A,
 135 B and C). Each reaction in this series was subjected to the same temperature sequence which was as
 136 follows: 250 → 350 → 450 °C. The only exception to this was Ca-Mo₂C's final temperature was 350°C
 137 because sampling at 250 °C would not have yielded useful data due to low conversion.



138
 139
 140
 141
 142
 143
 144
 145
 146
 147
 148
 149
 150
 151
 152 **Figure 3.** Product selectivity and of acetic acid conversion over three types of carbide pellet
 153 catalysts after pretreatment with 10% H₂ at 500 °C for 2 h: (A) Mo₂C, 4 h TOS; (B) Ni-Mo₂C, 4 h TOS;
 154 (C) Ca-Mo₂C, 4h TOS. (D) Yield of products at 450 °C over three types of carbide catalysts.

156 The un-doped catalyst produced mainly acetaldehyde at 250 °C and the conversion was low
 157 (~20%) [Figure 3 (A)]. As the reaction temperature increased to 350 and 450 °C the conversion
 158 improved. However, selectivity towards methane became dominant (45% at 450 °C) indicating
 159 increased contribution from the DCO pathway. Acetone, the ketonization product, was being
 160 produced over the un-doped carbide; however, the yield was only ~15% at 450 °C [Figure 3 (D)].

161 Ni-doped Mo₂C had highest selectivity towards aldehyde product at at 250 °C [Figure 3 (B)].
 162 This was consistent with the results seen from propionic acid hydrodeoxygenation. At higher
 163 temperatures methane and acetone became major products and the acetaldehyde selectivity was
 164 diminished similarly to the un-doped Mo₂C. Returning to the lower temperature again revealed that

165 catalyst deactivation had occurred to this catalyst also. Acetone selectivity was yet again enhanced in
 166 the catalyst's less active state. As described in the Catalyst Characterization section, the surface area
 167 and porosity of this catalyst did not experience any significant changes. Hydrogen activation
 168 property of carbides is known to suffer with surface oxygen accumulation, while oxygen-modified
 169 carbide surfaces present acid properties[15]. The observed deactivation could therefore be related to
 170 surface oxygen accumulation with TOS and temperature[14].

171 Ca-doped Mo₂C provided the highest acetone selectivity [Figure 3 (C)]. At 450 °C quantitative
 172 conversion was achieved with 94% selectivity towards the ketone. At lower temperatures
 173 acetaldehyde selectivity was dominant. Little selectivity towards light gases including methane was
 174 observed. Furthermore, the C2 and C3 products detected were purely alkene as shown in the olefin
 175 selectivity. This suggests that Ca-Mo₂C was less active in reactions involving H₂ activation such as
 176 acid hydrogenation, alkene hydrogenation, and hydrogenolysis. This property may arise from its
 177 "basic" nature. In one study looking at the decomposition of 2-propanol over Mo₂C, acetone
 178 selectivity was greatly enhanced by NH₃ poisoning[16,17]. This suggests that the basicity of the
 179 catalyst surface controls selectivity[16,17]. It has also been shown that both acid and basic sites exist
 180 on Mo₂C and modification of these sites can have a profound effect on reactivity.¹⁸

181 For better understanding the dopant effect on the acetic acid reactions, the total number of basic
 182 sites on three types of carbide catalysts were determined by temperature-programmed
 183 desorption of carbon dioxide (CO₂-TPD). The temperature for CO₂ desorption is usually an indication
 184 of the base site strength[18]. The amounts of CO₂ that desorbed from the carbide catalysts (Table 1)
 185 showed that Ca doped Mo₂C has the highest densities of basic sites (~1.77 micromoles/m²), which is
 186 more than double the amount for Mo₂C and Ni-Mo₂C. Our reaction data - Ca-Mo₂C showed the
 187 highest ketonization selectivity – suggests that basic sites were responsible for ketonization[19][20].
 188 Previous work has shown that the doped Mo₂C synthesis method can have a dramatic effect on the
 189 physical and chemical properties of the catalyst[21]. The surface properties of the carbide catalysts
 190 both before and after reaction are also summarized in Table 1. Metal doping (which was done before
 191 carburization) had a significant effect on the surface area of the resulting catalyst. The fresh catalysts,
 192 the un-doped, Ni-doped and Ca-doped had BET surface areas of 23.5, 18.3, and 9.55 m²/g,
 193 respectively. The addition of calcium had the greatest impact on surface area. It is believed that
 194 calcium slows the carburization process which leads to greater sintering, thus lowering the surface
 195 area[22]. The total pore volume followed a similar trend. The surface areas, post acetic acid
 196 hydrogenation, remained relatively unchanged, especially for Ca-Mo₂C. This suggests that the
 197 catalyst morphology was not greatly altered under our reaction conditions.

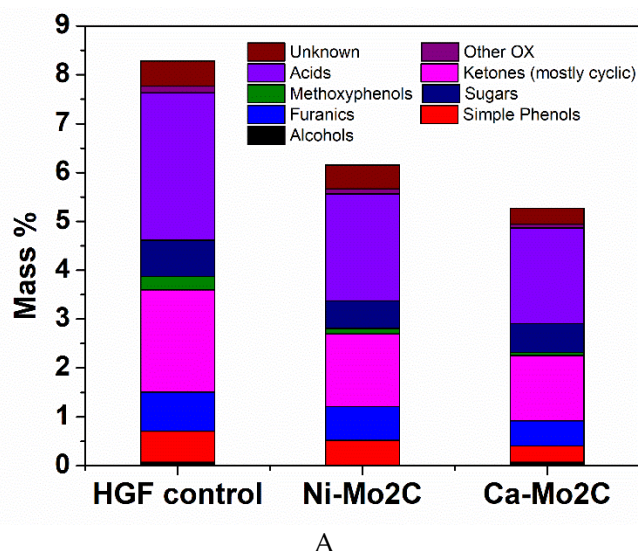
198
 199
 200

Table 1. Surface properties of three types of carbide catalysts.

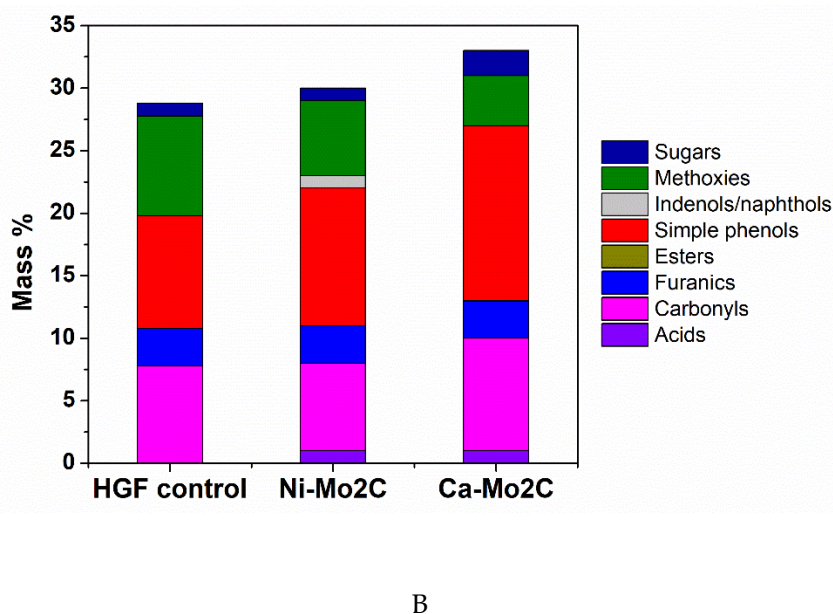
Catalyst	CO ₂ desorbed during TPD up to 550°C, micromoles/m ²	Surface Area, m ² /g	Surface Area after reaction*, m ² /g	Total Pore Volume, cm ³ /g	Total Pore Volume after reaction*, cm ³ /g	Average Pore Size, Å	Average Pore Size after reaction*, Å
Mo ₂ C	0.86	23.5	23.7	0.0925	0.0869	77.2	73.5
Ni-Mo ₂ C	0.79	18.3	17.2	0.0779	0.0701	85.2	81.4
Ca-Mo ₂ C	1.77	9.55	7.14	0.0375	0.0346	78.5	97.0

201 *Post reaction with Acetic Acid.

202
 203



204
205
206



207
208
209
210
211
212
213
214
215
216
217
218
219
220
221
222
223
224
225
226
227
228

Figure 4. Oxygenates products of real FP vapor over Ni and Ca doped carbide catalysts (CHGFs) compared with blank HGF sample in aqueous phase (A) and in organic phase (B).

The real FP vapor testing has been performed as shown in Figure 4. The goal of CHGF is to convert small carbonyl and carboxylic acid to more upgraded long chain chemicals. The products condensed into aqueous and organic phases, the aqueous products were analyzed by GC-FID and GC-MS, and organic phase products were analyzed by MBMS. In aqueous phase (Figure 4A), Ca-Mo₂C showed the greatest reduction in water soluble furanics, ketones, and most notably, acid content. From this analysis >99% of the acid content was acetic acid. Therefore, acetic acid decreased from 3% on HGF control sample to 1.9% on Ca-Mo₂C which is 36.7% reduction of acetic acid; and 2.19% on Ni-Mo₂C, which is 27% reduction of acetic acid. Also, the water-soluble ketone decreased from 2.09% on HGF control sample to 1.34% on Ca-Mo₂C, which is 37.5% reduction. Thus, we suppose these acetic acid and carbonyl compounds have been upgraded to chemicals with longer chains and went into the organic phase. These conclusions are further supported by the performance of the Ni-Mo₂C and Ca-Mo₂C CHGF catalysts for the organic phase results and compared with HGF control sample, shown in Figure 4B. Figure 4B summarizes oxygenates products in the organic phase (not soluble in water) which include long chain acids, carbonyls, furanics, esters, simple phenols, indenols/naphthols, methoxies, and sugars. Specifically, Simple Phenols are phenol, alkylphenols,

229 and catechols; methoxies are methoxy phenols and methoxy aromatics, furanics are
230 furans/benzofurans.

231 Regarding the total mass percent shown in y axis, this is a measure of GC analyzable content of
232 the organic non-water-soluble samples. The larger oxygenates that were either polymeric or have
233 more complicated functional groups did not make it through the column to the detector. By this
234 reasoning, a more upgraded product would have a greater mass% reported by the GC than a less
235 upgraded, or raw, pyrolysis product. Thus, the organic phase of real FP vapor over Ca-Mo₂C showed
236 the highest mass% (more GC analyzable compounds), indicating that the FP vapor was more
237 upgraded. For CHGF, the goal is to convert compounds that are less amenable to deoxygenation
238 reactions before they reach the primary upgrading reactor. The most problematic compound is
239 methoxy phenol, due to the high bond dissociation energy of the hydroxyl group, compared to cresol.
240 Ideally, a CHGF catalyst would convert these directly to product compounds like benzene, toluene
241 and xylene. Note that the methoxy phenols decreased from control HGF sample (8%) to CHGF
242 samples over Ni-Mo₂C (2.5%) and Ca-Mo₂C (4%). Meanwhile, simple phenols increased from control
243 HGF (9%) to CHGF samples over Ni-Mo₂C (10%) and Ca-Mo₂C (14%). Fortunately, these changes
244 were due to increased catechol production in Ni-Mo₂C (6%) and Ca-Mo₂C (4%) and increased
245 alkylphenols in Ni-Mo₂C (6%) and Ca-Mo₂C (8%) and not due to changes in phenol content, which
246 remained constant across treatments. Further, the carbonyl content of the control HGF sample was
247 similar to the Ni-Mo₂C (8%) while increasing under Ca-Mo₂C (10%) treatment. With respect to
248 aromatic content, the yields in the control HGF sample were low (0.3%), but the Ni-Mo₂C showed a
249 small decrease (0.2%) while the Ca-Mo₂C slightly increased (0.4%). Therefore Ca-Mo₂C loaded CHGF
250 showed the best upgrading performance by reducing 50% of less upgraded compounds into more
251 upgraded long chain phenols, carbonyls and aromatics.

252
253

254 3. Materials and Methods

255 **Materials:** The propionic acid ($\geq 99.5\%$), acetic acid ($> 99\%$), CaCl₂ and NiCl₂ were purchased from
256 Sigma-Aldrich and used as received. CH₄ (99.99%) and H₂ (99.999%) were purchased from AirGas;
257 MoO₃ and ammonium heptamolybdate powders were purchased from Alfa Aesar.

258 *Catalyst Synthesis and Characterization*

259 Carbide catalysts beads synthesis

260 The bulk Mo₂C catalysts used in this chapter were synthesized via a temperature-programmed
261 carburization (TPC) described previously[23]. The undoped Mo₂C was prepared using pressure-
262 pelletized heptamolybdate. To study the effects of metal doping on molybdenum carbide properties,
263 metal doped MoO₃ precursors were prepared before carburization. The precursors were prepared
264 via a gelation method[24]. In brief, MoO₃ powder was suspended in an aqueous solution of sodium
265 alginate. The oxide slurry was dropped into an aqueous solution of a metal chloride (CaCl₂ or NiCl₂).
266 The Na⁺ ions in the alginate binder exchanged with the divalent metal ions (e.g., one Ca²⁺ ion for two
267 Na⁺ ions) causing the alginate polymer molecules to cross-link. This process created a rigid MoO₃
268 bead.

269 The precipitated oxide beads were separated from solution, rinsed, dried, and heat-treated to 600 °C
270 for 2 h in air. Alginate was removed by calcining the particle leaving behind the doped MoO₃ beads.
271 Carburization was accomplished via the TPC method in a tubular quartz reactor of ~2.5 cm internal
272 diameter. During carburization, the oxygen was removed from molybdenum in the form of water
273 and carbon monoxide leaving behind Mo₂C. The carburizing gas consisted of 15% CH₄ and 85% H₂
274 (flow rate: 104 sccm per gram of precursor), the sample temperature was raised from room

275 temperature to 700 °C at 1 °C/min and held for 1 h. After cooling to room temperature, the
276 synthesized carbides were passivated in a 1% O₂/N₂ flow for 12 h.[25]

277 Specific Surface Area and pore size analysis (BET)

278 The morphology of carbides was analyzed via N₂ sorption using a Quantachrome Autosorb-1. The
279 samples were outgassed for 24 h at 400 °C prior to analysis. The total pore volume was measured at
280 (p/p₀=0.99) using Barrett-Joyner-Halenda (BJH) method. The pore size distribution was found using
281 19 point adsorption and 19 point desorption isotherms. The surface area was calculated from
282 adsorption points with p/p₀<0.35 per Brunauer-Emmett-Teller (BET) method.

283 Temperature programmed desorption of carbon dioxide (CO₂-TPD)

284 An Altamira AMI-200 characterization instrument was used for the measurements. The samples were
285 pretreated under 50 mL/min of 4% H₂/Ar for 3 h at approximately 500 °C, and then flushed in 50
286 mL/min of Ar for 30 min at the same temperature. After, the sample was cooled down to 30 °C under
287 50 mL/min of argon. Once at 30 °C, 45 mL/min of 2% CO₂/Ar were flowed through the sample for 1
288 h. The gas flowing through the sample was switched to 45 mL/min of argon and 1 h was allowed for
289 weakly bound CO₂ species to desorb before the temperature programmed desorption (TPD)
290 experiment was started. For the TPD experiment, 45mL/min of argon were used as the carrier gas.
291 The temperature was ramped from 30 °C to 1000 °C at a rate of 10 °C/min, and then held at 1000°C
292 for 1 h. The CO₂ desorbed was analyzed using a mass spectrometer.

293 *Catalysts Testing*

294 Acid hydrodeoxygenation experiments were conducted using a bench-top flow through reactor
295 system. The product selectivity and reactant conversion were measured as a function of temperature
296 and time on stream (TOS). These experiments were run under atmospheric pressure. In a typical test,
297 400 mg of catalyst was packed in a 1 cm I.D. quartz tube. After loading the catalyst, the bed was
298 heated to 500 °C at a rate of 5 °C/min under 45 sccm helium. At 500 °C, 5 sccm H₂ was added to the
299 helium stream. The pretreatment was continued for 2 hours before cooling the reactor to a desired
300 reaction temperature (e.g, 250 or 350 °C) at a rate of ~10°C/min. The carboxylic acid was introduced
301 into the reactor by redirecting H₂-He gas through a bubbler/saturator with an average flow of 0.15
302 ml/h affording an effective space velocity of 0.37 h⁻¹ WHSV (acid basis). The exit vapor was analyzed
303 by directly injecting to either the GC-FID for product quantification or GC-MS for product
304 identification. After the 1st injection, the reactor temperature was increased and allowed to equilibrate
305 for an hour. This was again repeated and after the third injection the reactor was cooled to the initial
306 temperature. Another sample was taken after an hour of equilibration. The fourth injection was
307 meant to assess the stability of the material over the 4 hours of operation.

308 *FP real vapor testing*

309 Catalytic hot gas filtration of pine pyrolysis vapors was carried out on a 40 g/hr slipstream from the
310 NREL Vapor Phase Upgrading unit. The filter units were a scaled down version of the Pall
311 Diaschumalith filter elements with a gas filtration grade of 0.3 µm. The filter support is constructed
312 from SiC with an outer alumina (mullite) membrane. The filter ends were kaolin-sealed to prevent
313 vapor bypassing and mounted in a 316SS filter housing with flow passing from the outside of the
314 membrane into the interior of the filter. Empty filters were used for the control and 1g catalyst
315 beads or pellets were packed into the interior of the filter with quartz wool at either end, to give a
316 WHSV of 23 hr⁻¹ of pine pyrolysis vapor. Inert SiC chips were employed to fill the additional filter
317 volume. The output of the CHGF filter was further analyzed by MBMS and then condensed to
318 liquid product and the remaining volumetric flow of product gas was measured by means of a dry
319 test meter and the carbon content analyzed by an HP5890 GC with an Activated Research PolyArc

320 and FID. The CHGF filters were weighed on a high-precision Mettler-Toledo balance before and
321 after the experiment to quantify the mass of coke deposited on the filter and the catalyst bed.

322 4. Conclusions

323 We have shown that un-doped Mo₂C is active towards both acetic and propionic acid
324 hydrodeoxygenation under atmospheric pressure. Additionally, we found that doping the MoO₃
325 with Ni or Ca prior to carburization can have dramatic effects on the physical characteristics as well
326 as the reactivity of the resulting carbides. Ni-Mo₂C was found to be more active towards
327 hydrogenation than the other catalysts. Ca-Mo₂C was found to exhibit superior selectivity (94%) for
328 the acetone production especially at high temperatures relevant to pyrolysis vapor upgrading, e.g.,
329 450 °C. Overall, the reactivity trends observed on a given catalyst type was consistent between acetic
330 and propionic acids. Carbide catalysts particularly Ca-doped one were shown to effectively upgrade
331 the real FP vapor as well. Thus, carbide catalysts appear promising for deoxygenation of bio-derived
332 compounds with possibility of tailoring product selectivity via metal doping. Further catalyst
333 characterization would be useful to understand the deactivation pathways, which could provide
334 insight into the nature of the various active sites. This information would aid in designing the
335 physical and chemical properties of these materials to achieve greater conversions, enhanced
336 selectivity and extended durability.

337 **Acknowledgments:** DOE BETO office and Beth Armstrong at ORNL for help with the doped MoO₃ beads
338 synthesis.

339 **Author Contributions:** M.L. A.L., J.-S.C. and M.Z.H conceived and designed the experiments; M.L. and A.L.
340 performed the experiments; M.L., A.L and M.J. analyzed the data; Z.L., K.M., B.P., Z.W and F.P contributed
341 during experiments and discussion; M.L. and A.L wrote the paper with contribution from the other co-authors."

342 **Conflicts of Interest:** The authors declare no conflict of interest.

343 References

- 344 1. Baldwin, R. M.; Feik, C. J. Bio-oil stabilization and upgrading by hot gas filtration. *Energy and*
345 *Fuels* **2013**, *27*, 3224–3238, doi:10.1021/ef400177t.
- 346 2. Wang, H.; Male, J.; Wang, Y. Recent advances in hydrotreating of pyrolysis bio-oil and its
347 oxygen-containing model compounds. *ACS Catalysis* **2013**, *3*, 1047–1070,
348 doi:10.1021/cs400069z.
- 349 3. Huber, G. W.; Corma, A. Synergies between bio- and oil refineries for the production of fuels
350 from biomass. *Angewandte Chemie - International Edition* **2007**, *46*, 7184–7201,
351 doi:10.1002/anie.200604504.
- 352 4. Pallassana, V.; Neurock, M. Reaction paths in the hydrogenolysis of acetic acid to ethanol over
353 Pd(111), Re(0001), and PdRe alloys. *Journal of Catalysis* **2002**, *209*, 289–305,
354 doi:10.1006/jcat.2002.3585.
- 355 5. Nguyen, M. T.; Sengupta, D.; Raspoet, G.; Vanquickenborne, L. G. Theoretical study of the
356 thermal decomposition of acetic acid: Decarboxylation versus dehydration. *Journal of Physical*
357 *Chemistry* **1995**, *99*, 11883–11888, doi:10.1021/j100031a015.
- 358 6. Pestman, R.; Koster, R. M.; Van Duijine, A.; Pieterse, J. A. Z.; Ponec, V. Reactions of carboxylic
359 acids on oxides: 2. Bimolecular reaction of aliphatic acids to ketones. *Journal of Catalysis* **1997**,
360 *168*, 265–272, doi:10.1006/jcat.1997.1624.

- 361 7. Martinez, R.; Huff, M. C.; Barteau, M. A. Ketonization of acetic acid on titania-functionalized
362 silica monoliths. *Journal of Catalysis* **2004**, *222*, 404–409, doi:10.1016/j.jcat.2003.12.002.
- 363 8. He, D. H.; Wakasa, N.; Fuchikami, T. Hydrogenation of carboxylic acids using bimetallic
364 catalysts consisting of group 8 to 10, and group 6 or 7 metals. *Tetrahedron Letters* **1995**, *36*, 1059–
365 1062, doi:10.1016/0040-4039(94)02453-I.
- 366 9. Cheah, K. Y.; Tang, T. S.; Mizukami, F.; Niwa, S. ichi; Toba, M.; Choo, Y. M. Selective
367 hydrogenation of oleic acid to 9-octadecen-1-ol: Catalyst preparation and optimum reaction
368 conditions. *Journal of the American Oil Chemists' Society* **1992**, *69*, 410–416,
369 doi:10.1007/BF02540940.
- 370 10. Ji, N.; Zhang, T.; Zheng, M.; Wang, A.; Wang, H.; Wang, X.; Chen, J. G. Direct catalytic
371 conversion of cellulose into ethylene glycol using nickel-promoted tungsten carbide catalysts.
372 *Angewandte Chemie - International Edition* **2008**, *47*, 8510–8513, doi:10.1002/anie.200803233.
- 373 11. Ren, H.; Yu, W.; Saliccioli, M.; Chen, Y.; Huang, Y.; Xiong, K.; Vlachos, D. G.; Chen, J. G.
374 Selective hydrodeoxygenation of biomass-derived oxygenates to unsaturated hydrocarbons
375 using molybdenum carbide catalysts. *ChemSusChem* **2013**, *6*, 798–801,
376 doi:10.1002/cssc.201200991.
- 377 12. Xiong, K.; Yu, W.; Vlachos, D. G.; Chen, J. G. Reaction pathways of biomass-derived
378 oxygenates over metals and carbides: From model surfaces to supported catalysts.
379 *ChemCatChem* **2015**, *7*, 1402–1421, doi:10.1002/cctc.201403067.
- 380 13. Jongerius, A. L.; Gosselink, R. W.; Dijkstra, J.; Bitter, J. H.; Bruijninx, P. C. A.; Weckhuysen,
381 B. M. Carbon nanofiber supported transition-metal carbide catalysts for the
382 hydrodeoxygenation of guaiacol. *ChemCatChem* **2013**, *5*, 2964–2972,
383 doi:10.1002/cctc.201300280.
- 384 14. Sullivan, M. M.; Chen, C. J.; Bhan, A. Catalytic deoxygenation on transition metal carbide
385 catalysts. *Catalysis Science and Technology* **2016**, *6*, 602–616, doi:10.1039/c5cy01665g.
- 386 15. Sullivan, M. M.; Bhan, A. Acetone Hydrodeoxygenation over Bifunctional Metallic-Acidic
387 Molybdenum Carbide Catalysts. *ACS Catalysis* **2016**, *6*, 1145–1152,
388 doi:10.1021/acscatal.5b02656.
- 389 16. Bej, S. K.; Bennett, C. A.; Thompson, L. T. Acid and base characteristics of molybdenum
390 carbide catalysts. *Applied Catalysis A: General* **2003**, *250*, 197–208, doi:10.1016/S0926-
391 860X(02)00664-6.
- 392 17. Bej, S. K.; Thompson, L. T. Acetone condensation over molybdenum nitride and carbide
393 catalysts. *Applied Catalysis A: General* **2004**, *264*, 141–150, doi:10.1016/j.apcata.2003.12.051.
- 394 18. Hattori, H. Heterogeneous Basic Catalysis. *Chemical Reviews* **1995**, *95*, 537–558,
395 doi:10.1021/cr00035a005.

- 396 19. Hendren, T. S.; Dooley, K. M. Kinetics of catalyzed acid/acid and acid/aldehyde condensation
397 reactions to non-symmetric ketones. *Catalysis Today* **2003**, *85*, 333–351, doi:10.1016/S0920-
398 5861(03)00399-7.
- 399 20. Mante, O. D.; Rodriguez, J. A.; Senanayake, S. D.; Babu, S. P. Catalytic conversion of biomass
400 pyrolysis vapors into hydrocarbon fuel precursors. *Green Chemistry* **2015**, *17*, 2362–2368,
401 doi:10.1039/c4gc02238f.
- 402 21. Han, J.; Duan, J.; Chen, P.; Lou, H.; Zheng, X.; Hong, H. Carbon-supported molybdenum
403 carbide catalysts for the conversion of vegetable oils. *ChemSusChem* **2012**, *5*, 727–733,
404 doi:10.1002/cssc.201100476.
- 405 22. Jung, K. T.; Kim, W. B.; Rhee, C. H.; Lee, J. S. Effects of Transition Metal Addition on the Solid-
406 State Transformation of Molybdenum Trioxide to Molybdenum Carbides. *Chemistry of*
407 *Materials* **2004**, *16*, 307–314, doi:10.1021/cm030395w.
- 408 23. J. S. Lee, S. T. O. and M. B. Molybdenum carbide catalysts. I Synthesis of unsupported
409 powders. *Journal of catalysis* **1987**, *106*, 125–133, doi:0021-9517/87.
- 410 24. Lundberg, D. Flow Conditioners. *Control Engineering* **2006**, *53*, 2–7, doi:10.1016/j.(73).
- 411 25. Choi, J. S.; Zacher, A. H.; Wang, H.; Olarte, M. V.; Armstrong, B. L.; Meyer, H. M.; Soykal, I.
412 I.; Schwartz, V. Molybdenum Carbides, Active and in Situ Regenerable Catalysts in
413 Hydroprocessing of Fast Pyrolysis Bio-Oil. *Energy and Fuels* **2016**, *30*, 5016–5026,
414 doi:10.1021/acs.energyfuels.6b00937.
- 415
- 416